J Mater Sci (2016) 51:861–867
DOI 10.1007/s10853-015-9410-5

Synthesis of cellulose-derived carbon dots using acidic ionic liquid as a catalyst and its application for detection of Hg^{2+}

Congyue Wang[1] · Chunfeng Wang[1] · Panpan Xu[1] · Aoqi Li[1] · Yujuan Chen[1] · Kelei Zhuo[1]

Received: 9 June 2015 / Accepted: 3 September 2015 / Published online: 9 September 2015

Abstract Carbon dots (CDs) as versatile carbon-based nanomaterials have attracted increasing attention because of their non-toxicity, good water solubility and photostability, and easy surface functionalization. For their wide application, it is still needed to explore moderate and facile methods for synthesizing CDs from green and inexpensive precursors. In this paper, a moderate method was developed to synthesize water-soluble CDs by ionothermal treatment of cellulose with SO_3H-functionalized acidic ionic liquid as a catalyst in 1-butyl-3-methylimidazolium chloride ([Bmim]Cl). The preparation process was carried out at relatively low temperature in non-pressurized vessel. The synthesized CDs exhibit near-spherical morphology with an average diameter of 8.0 nm, and the surface is carbon and oxygen rich. The CDs have powder-blue fluorescence with excitation-dependent emission behavior and excellent stability. Moreover, the as-prepared CDs were demonstrated as an effective "turn-off" fluorescent probe for the selective detection of Hg^{2+} with a good linear relationship over the concentration range from 6 to 80 μM. The application of acidic ionic liquid should provide a new path for the synthesis of CDs under mild condition.

✉ Kelei Zhuo
klzhuo@263.net

[1] Collaborative Innovation Center of Henan Province for Green Manufacturing of Fine Chemicals, Key Laboratory of Green Chemical Media and Reactions, Ministry of Education, School of Chemistry and Chemical Engineering, Henan Normal University, Xinxiang 453007, Henan, People's Republic of China

Introduction

As a versatile carbon nanomaterial, carbon dots (CDs) have many fascinating properties such as non-toxicity, chemical stability, and unique fluorescence [1, 2]. Thus they have shown great potential in bioimaging [3–5], photocatalysis [6], electrocatalysis [7], and chemical sensing [8–11]. In 2004, CDs were first discovered accidentally during the separation and purification of single-walled carbon nanotubes [12]. Since then, this new class of carbon nanomaterials has garnered much focus of researchers, and various synthesis methods have been demonstrated for the preparation of CDs. Up to now, the main synthesis methods for the preparation of CDs consist of hydrothermal or solvothermal treatment [13], chemical ablation [3, 14], microware irradiation [15], ultrasonic treatment [16], laser ablation [17], and electrochemical carbonization [18]. However, all the approaches above-mentioned suffer from several drawbacks such as drastic processes, time consuming, and expensive precursors [2], which limit the large-scale preparation and wide application of CDs. Therefore, novel moderate and facile methods for synthesizing CDs from green and inexpensive precursors still need to be explored.

Ionic liquids (ILs) as an attractive "green solvent" have many unique properties, including high polarity, negligible vapor pressure, a wide electrochemical window, and good thermal stability. These properties make ILs have many advantages in the fabrication of the nanomaterials [19]. In recent years, ILs have been used to synthesize nanostructured metal materials [20] and other inorganic nanomaterials [21]. In 2009, Lu and co-authors reported the fabrication of nanoparticles from graphite electrode using ionic liquid-assisted electrochemical exfoliation [22]. Size-controlled CDs were synthesized through adjusting the

applied voltages on the electrodes in the mixed electrolyte containing ILs and water [23]. Besides, ILs can also be used as precursors [24] and capping agent [25] for the preparation of CDs. However, the application of acidic ionic liquid in the preparation of CDs remains less studied until now. Acidic ionic liquid, which combined the advantages of mineral acid and ionic liquid, is an environmentally benign catalyst for many organic reactions, such as esterification, polymerization, and carbonylation [26]. This catalyst may also be useful in the synthesis of CDs and makes the preparation process become mild.

Herein, 1-butyl-3-methylimidazolium chloride ([Bmim]Cl) as a solvent and SO_3H-functionalized acidic ionic liquid (SO_3H-IL) as a catalyst were used for the preparation of CDs from microcrystalline cellulose (MCC) in this work. Because of the presence of acidic ionic liquid, cellulose could be carbonized at relatively low temperature and atmospheric pressure. The obtained CDs have excellent water solubility and photostability. In addition, the CDs had fluorescent response to Hg^{2+} and could be used as "turn-off" fluorescent probe for monitoring Hg^{2+} in aqueous solution.

Materials and methods

Materials

Microcrystalline cellulose (MCC, average particle size of 50 μm) and 1-butyl-3-methylimidazolium chloride ([Bmim]Cl, CP, >99 %) were purchased from J&K Chemical Company (Beijing, China). $CaCl_2$, $Hg(NO_3)_2 \cdot H_2O$, $MgCl_2$, $CuCl_2$, $Co(NO_3)_2$, $BaCl_2$, $CdCl_2$, and $NiCl_2$ were purchased from Beijing Chemical Corp. $MnCl_2$, $Pb(NO_3)_2$, and $FeCl_3$ were purchased from Tianjin Chemical Corp. All the chemicals are of analytical grade and used as received without further purification. And all the aqueous solutions were prepared using doubly deionized water.

Synthesis of CDs

SO_3H-functionalized acidic ionic liquid (1-(1-propylsulfonic)-3-methylimidazolium hydrogen sulfate) was synthesized according to the previously reported method [27]. For the preparation of CDs, MCC (0.3 g) and [Bmim]Cl (4.0 g) were added into a 50-mL round-bottom flask and stirred for 1 h at 100 °C until the transparent and homogeneous solution was obtained. Then the as-prepared SO_3H-IL (0.4 g) was added to the reaction system and reacted for 4 h under stirring at 80 °C. The obtained dark sticky mixture was diluted with doubly deionized water and centrifuged for 10 min at 2000 rpm to remove the black precipitates. Then the supernatant was filtered through a 0.22-μm microporous membrane, and the obtained dark yellow CDs dispersion was dialyzed with a molecular weight cutoff of 500 Da for 24 h to remove ILs and other small molecular compounds.

Characterization

Ultraviolet–visible (UV–Vis) absorption and photoluminescence (PL) spectra were measured with a TU-1900 UV–vis spectrophotometer (Beijing Purkinje) and FP-6500 fluorescence spectrophotometer (Jasco, Japan), respectively. Fourier transform infrared (FTIR) spectrum of CDs was recorded on a Nicolet 6700 spectrophotometer (Nicolet) using KBr pressed disks. The high-resolution transmission electron microscopy (HRTEM) image was obtained with a JEOL 2010 electron microscope at an accelerating voltage of 200 kV. The X-ray photoelectron spectroscopy (XPS) measurements were made using a Thermo Scientific K-Alpha electron energy spectrometer using Al Ka (1486.6 eV) as the X-ray excitation source. Binding energy for C1s at 284.6 eV is standard. The absolute quantum yield (QY) and fluorescence lifetime of CDs were measured by FLS980 (Edinburgh Instruments Ltd., British) fluorescence spectrometer.

Detection of Hg^{2+}

Detection of Hg^{2+} in pure water was performed in phosphate buffer solution (PBS, 10 mM, pH 7.0) at room temperature. In a typical assay, 40 μL of CDs solution was added to 1 mL of PBS. Then a calculated amount of Hg^{2+} was mixed together with the aqueous solution containing the same amount of CDs and reacted for 20 min before spectral measurements. To confirm the selectivity for Hg^{2+}, the PL intensities of CDs with other metal ions including Cu^{2+}, Co^{2+}, Ca^{2+}, Mn^{2+}, Ni^{2+}, Mg^{2+}, Cd^{2+}, Ba^{2+}, Fe^{3+}, and Pb^{2+} were inspected in the similar way.

Results and discussion

In the present reaction system, for the low-cost preparation of CDs, cellulose (the most abundant biorenewable material on Earth) was selected as a raw material. However, cellulose is difficult to be dissolved in water and common organic solvents [28]. [Bmim]Cl, which can form hydrogen-bonding networks between hydroxyl groups of cellulose and chloride ions [29], is a good solvent for the dissolution of cellulose. SO_3H-IL is a benign catalyst for hydrolysis of cellulose owing to high catalytic activity for the fracture of glycosidic bonds. Additionally, SO_3H-IL is also an excellent catalyst for many organic reactions, such

as esterification, polymerization, carbonylation, aldol condensation, etc. [26]. Hence, these two ILs were selected as solvent and catalyst in this study and the preparation process of CDs is illustrated in Fig. 1. The potential mechanism for the formation of CDs may involve two steps: Firstly, hydrolysis of cellulose took place in the presence of SO_3H-IL after dissolution of cellulose in [Bmim]Cl, generating sugars and some oligomers, some of which subsequently dehydrated to acids, aldehydes, phenols, etc. [30, 31]. Secondly, these products reacted with each other under the catalysis of SO_3H-IL to produce soluble polymers which further developed into CDs after the consecutive processes of polymerization, aromatization, and ultimately generation and growth of carbogenic nuclei [32, 33]. For comparison, the experiments without adding SO_3H-IL were carried out. There was no distinct carbonation phenomenon for cellulose even after reaction for 4 h at 150 °C.

To find the optimal reaction condition, we investigated the fluorescence spectra of resultant CDs under different reaction ratios and temperatures. The results indicated that reaction ratio and temperature have no obvious impact on the fluorescent properties of the resultant CDs in our experiments, but they have an effect on carbonation speed of cellulose. In order to use ILs effectively and synthesize CDs in short time and at low temperature, a mass ratio of [Bmim]Cl/cellulose/SO_3H-IL of 4.0/0.3/0.4 and a reaction temperature of 80 °C were selected as the optimal reaction condition.

TEM image (Fig. 2a) shows that most of the obtained CDs exhibit well-dispersed near-spherical morphology. The diameters of most of the obtained CDs are distributed in the range of 3–13.5 nm (Fig. 2b) and with an average diameter value of 8.0 nm (100 random nanoparticles were selected for the sample). The high-resolution TEM image (HRTEM) reveals that CDs have crystalline structure with lattice fringe of 0.32 nm (the inset image of Fig. 2a).

In the FTIR spectrum (Fig. 3a), there is a broad and intense peak at around 3380 cm^{-1} which corresponds to the stretching vibration of O–H and N–H. The peaks at 2961, 2875, and 1401 cm^{-1} indicate the existence of C–H bond. The peaks at 1573 and 1123 cm^{-1} are due to the stretching vibration of C=C and C–O–C, respectively.

The surface composition and chemical state of the as-prepared CDs were further investigated by X-ray photoelectron spectroscopy (XPS). The full-scan XPS spectrum (Fig. 3b) has four peaks at 532.41, 401.61, 284.83, and 167.89 eV, corresponding to C_{1s}, O_{1s}, N_{1s}, and S_{2p}, respectively. The elemental contents of sample are 71.51 % (C), 22.47 % (O), 4.33 % (N), and 1.69 % (S). The results reveal that besides abundant carbon and oxygen, the surface of obtained CDs also contains a small amount of nitrogen and sulfur. The carbon and oxygen may mainly come from cellulose, while nitrogen and sulfur may come from the ILs adsorbed on the CDs' surface. The high-resolution XPS spectra of the C_{1s}, O_{1s}, N_{1s}, and S_{2p} are shown in Fig. 4. In the high-resolution C_{1s} spectrum (Fig. 4a), the signals of five distinct carbon states C–C/C=C, C–S, C–N, C–O, and C=O present at 284.444, 284.8, 285.188, 286.245, and 287.551 eV, respectively [14]. The O_{1s} spectrum shown in Fig. 4b has two peaks at 531.901 and 532.615 eV, which are attributed to C=O and C–OH/C–O–C groups, respectively. The high-resolution N_{1s} spectrum (Fig. 4c) can be deconvoluted into two peaks at 399.5 and 401.635 eV, which represent N_{1s} states in C=N and C–N [34]. The deconvoluted peaks at 167.529, 168.223, and 168.933 eV in the S_{2p} spectrum (Fig. 4d) indicate that sulfur exists mostly in the form of –C–SO_x– ($x = 2, 3, 4$) [9]. The analysis of FTIR and XPS spectra shows that the surface of the as-synthesized CDs has multiple oxygenated groups like –COOH and –OH.

To further explore their optical properties, the UV–Vis absorption and photoluminescence (PL) spectra of CDs were measured and are shown in Fig. 5a. Two obvious absorption peaks centering at 210 and 276 nm were seen in the UV–Vis absorption spectrum, which should be ascribed to n–π^* transition of C=O and π–π^* transition of C=C [35]. The synthesized CDs have excitation-dependent emission behavior (Fig. 5b), and the intensity of PL emission peak at 450 nm is the highest when excitation wavelength is 360 nm. The photographs (inset in Fig. 5a) show that the aqueous solution of CDs emitted powder-blue fluorescence under 365 nm UV light (right) while appearing as yellow under room light (left). The absolute quantum yield (QY) of CDs was measured to be 4.7 % using an integrating sphere attached to an FLS980 fluorescence spectrometer.

The photochemical stability of CDs at different conditions was also investigated by recording the PL intensities of CDs at different ionic strengths, pH values, and irradiation times under UV lamp. As shown in Fig. 6a, the PL intensities remain unchanged at different ionic strengths regulated by concentrations of NaCl. Therefore, the CDs

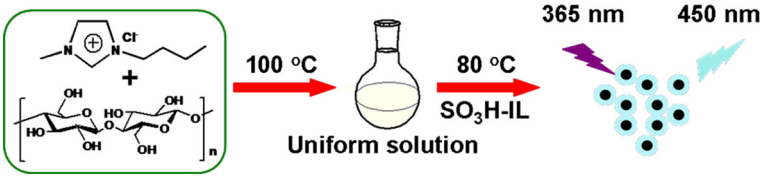

Fig. 1 The diagram of preparation process for CDs

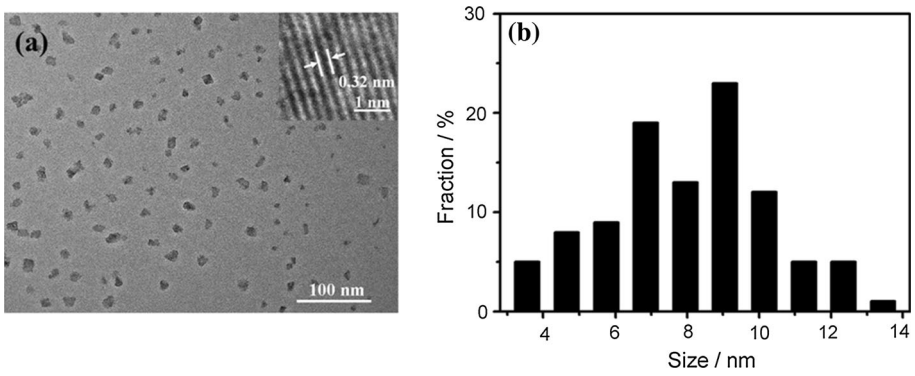

Fig. 2 **a** TEM image of CDs, *inset*: HRTEM image of single CD; **b** the particle size distribution histogram of CDs

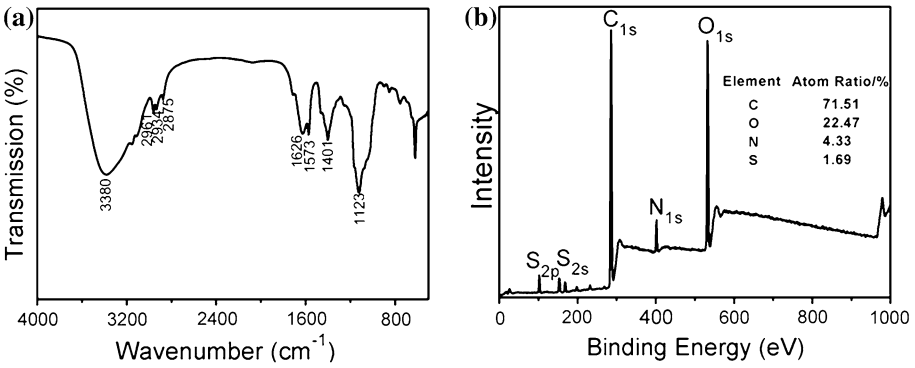

Fig. 3 **a** FTIR spectrum and **b** XPS full-scan spectrum of CDs

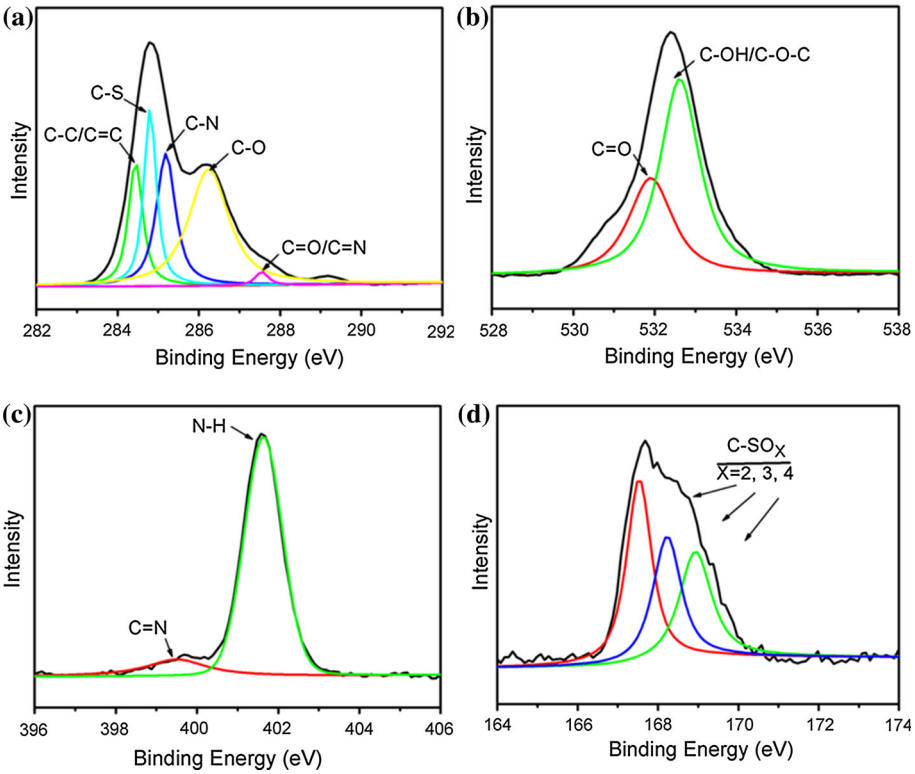

Fig. 4 High-resolution XPS spectra of **a** C_{1s}, **b** O_{1s}, **c** N_{1s}, and **d** S_{2p}

have excellent stability when exposed to environments with high ionic strengths. The effect of UV irradiation time on PL intensity is shown in Fig. 6b. A slight decrease of the PL intensity of CDs is observed during continuous exposure of 100 min, which demonstrates that the surface states of CDs are unstable when exposed to UV lamp

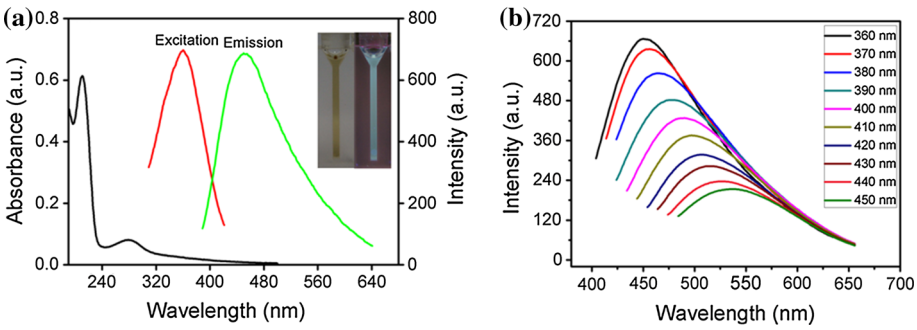

Fig. 5 **a** The UV–Vis absorption, PL excitation, and emission spectra of CDs, *insets*: photographs of CDs under room light (*left*) and 365 nm UV lamp (*right*) of CDs aqueous solution; **b** PL emission spectra of CDs aqueous solution at an excitation wavelength from 360 to 450 nm

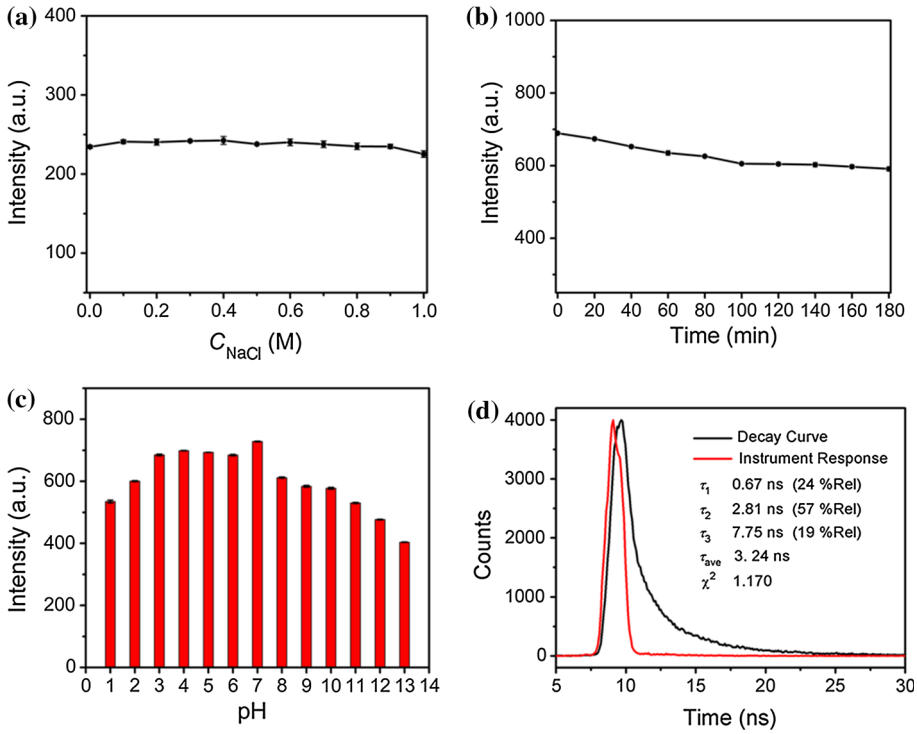

Fig. 6 **a** The PL intensity of CDs at different ionic strengths regulated by concentrations of NaCl from 0 to 1 M; **b** the PL intensity of CDs at different irradiation times with an UV lamp; **c** the effect of pH value on PL intensity of CDs; and **d** the fluorescence lifetime of CDs

during this time. However, CDs have resistance to photobleaching in some degree, because PL intensities are unchanged with the irradiation time from 100 to 180 min. The PL intensities of CD in various pH values from 1 to 13 are given in Fig. 6c. Overall, PL intensity is stronger in the acidic condition than under alkaline conditions and reach the highest at pH 7. This result is similar to that reported in the literature [36], which is perhaps owing to the variation of functional groups on the surface of CD at different pH values. The PL intensity of CDs is higher in the pH range from 3 to 7 than in other pH values, indicating that they have more application potential in acidic and neutral conditions.

At present, although the actual PL mechanism of CDs is still not yet entirely clear, there is mounting evidence that emission arises from both an intrinsic band gap resulting from confined sp^2 conjugation in the core of CDs and the surface state that can be excited either directly or by energy transfer from an intrinsic band [37]. The luminescence decay profile of the CDs excited at 360 nm was recorded using a time-correlated single-photon counting technique (Fig. 6d). The data of fluorescence lifetime are very well fitted to a triple exponential, and the average fluorescence lifetime was calculated to be 3.24 ns. Such a short lifetime demonstrates that the possible luminescent mechanism is the radioactive recombination of excitations [38].

To evaluate the feasibility sensitivity of the CDs as sensors monitoring Hg^{2+} in aqueous solutions, the PL intensities of CDs with different concentrations of Hg^{2+} in PBS (pH 7) were studied. The PL emission spectra of CDs with different concentrations of Hg^{2+} in the range of 0–80 μM (Fig. 7a) reveal that PL intensity of CDs at 450 nm decreases gradually with the increase of concentration of Hg^{2+}. This suggests that Hg^{2+} can effectively quench the

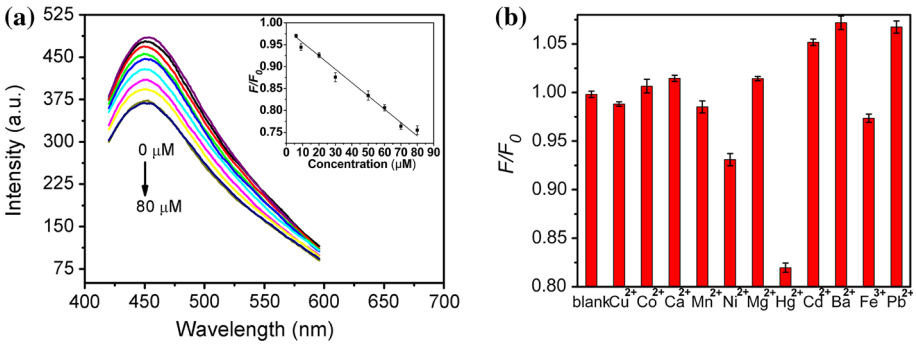

Fig. 7 **a** PL emission spectra of CDs with different concentrations of Hg^{2+} (0, 5, 6, 9, 20, 30, 50, 60, 70, and 80 μM) in PBS (10 mM, pH 7) at an excitation of 355 nm, *inset*: relative fluorescence intensity (F/F_0) versus concentration of Hg^{2+} (from 6 to 80 μM); **b** the PL response of CDs to various metal ions including Cu^{2+}, Co^{2+}, Ca^{2+}, Mn^{2+}, Ni^{2+}, Mg^{2+}, Hg^{2+}, Cd^{2+}, Ba^{2+}, Fe^{3+}, and Pb^{2+} in PBS (10 mM, pH 7). F and F_0 correspond to the fluorescence intensities of the CDs with and without 60 mM of different metal ions, respectively

fluorescence of CDs, which may be ascribed to the non-radiative electron transfer from the excited state to the d-orbital of Hg^{2+} [39]. The relative PL intensities (F/F_0) displayed a good linear relationship versus the concentration of Hg^{2+} in the range of 6–80 μM (inset in Fig. 7a) with a linear equation of $F/F_0 = -0.00301c + 0.98315$ ($R^2 = 0.9863$), where c is the concentration of Hg^{2+}, and F and F_0 are FL intensities at 450 nm in the presence and absence of Hg^{2+}, respectively. Furthermore, the relative standard deviation (RSD) was 1.02 % for five repeated measurements of 60 μM Hg^{2+}, showing an excellent reproducibility of these fluorescent sensors. The limit of detection (calculated according to a signal-to-noise ratio of S/N = 3) was estimated to be 1.6 μM, which is higher than the acceptable value mandated by the EPA for drinking water. However, the sensors can be useful in detecting inorganic mercury in samples of biological products, drugs, fish, and also in samples where regulations for mercury are less stringent [40].

We have also evaluated the selectivity of this analytical system. The obtained CDs have more obvious fluorescence quenching in the presence of Hg^{2+} than other metal ions including Cu^{2+}, Co^{2+}, Ca^{2+}, Mn^{2+}, Ni^{2+}, Mg^{2+}, Cd^{2+}, Ba^{2+}, Fe^{3+}, and Pb^{2+} (Fig. 7b). This phenomenon indicates that the CDs have selectivity for Hg^{2+}, which may due to the factor that the carboxylic and hydroxyl on the surfaces of the CDs have stronger affinity to Hg^{2+} than to other metal ions.

Conclusion

We developed a moderate method for the preparation of fluorescent CDs from cellulose (green, low-cost, and commonly available biomass) using [Bmim]Cl as a solvent and SO_3H-functionalized acidic ionic liquid as a catalyst. The obtained CDs have good water solubility, excitation-dependent emission behavior, excellent stability in high ionic strength, and resistance to photobleaching. The as-prepared CDs, with any surface functionalization, have a certain degree of sensitivity and selectivity for Hg^{2+}, indicating that the CDs have potential to be used as "turn-off" fluorescent sensors for the detection of Hg^{2+} in aqueous solution.

Acknowledgements Financial support from the National Natural Science Foundation of China (No. 21173070, 21303044) is gratefully acknowledged.

References

1. Baker SN, Baker GA (2010) Luminescent carbon nanodots: emergent nanolights. Angew Chem Int Ed 49:6726–6744
2. Wang YF, Hu AG (2014) Carbon quantum dots: synthesis, properties and applications. J Mater Chem C 2:6921–6939
3. Shen LM, Zhang LP, Chen ML, Chen XW, Wang JH (2013) The production of pH-sensitive photoluminescent carbon nanoparticles by the carbonization of polyethylenimine and their use for bioimaging. Carbon 55:343–349
4. Huang H, Li CG, Zhu SJ, Wang HL, Chen CL, Wang ZR, Bai TY, Shi Z, Feng SH (2014) Histidine-derived nontoxic nitrogen-doped carbon dots for sensing and bioimaging applications. Langmuir 30:13542–13548
5. Gong XJ, Lu WJ, Paau MC, Hub Qin, Xin Wu, Shuang SM, Dong C, Choi MMF (2015) Facile synthesis of nitrogen-doped carbon dots for Fe^{3+} sensing and cellular imaging. Anal Chim Acta 861:74–84
6. Hu SL, Tian RX, Dong YG, Yang JL, Liu J, Chang Q (2013) Modulation and effects of surface groups on photoluminescence and photocatalytic activity of carbon dots. Nanoscale 5:11665–11671
7. Gao SY, Chen YL, Fan H, Wei XJ, Hu CG, Wang LX, Qu LT (2014) A green one-arrow-two-hawks strategy for nitrogen-doped carbon dots as fluorescent ink and oxygen reduction electrocatalysts. J Mater Chem A 2:6320–6325
8. Hu C, Yu C, Li MY, Wang XN, Yang JY, Zhao ZB, Eychmüller A, Sun YP, Qiu JS (2014) Chemically tailoring coal to fluorescent carbon dots with tuned size and their capacity for Cu(II) detection. Small 10:4926–4933

9. Hu YP, Yang J, Tian JW, Jia L, Yu JS (2014) Waste frying oil as a precursor for one-step synthesis of sulfur-doped carbon dots with pH-sensitive photoluminescence. Carbon 77:775–782
10. Wang CX, Xu ZZ, Cheng H, Lin HH, Humphrey MG, Zhang C (2015) A hydrothermal route to water-stable luminescent carbon dots as nanosensors for pH and temperature. Carbon 82:87–95
11. Xu Q, Zhao JG, Liu Y, Pu P, Wang XS, Chen YS, Gao C, Chen JR, Zhou HJ (2015) Enhancing the luminescence of carbon dots by doping nitrogen element and its application in the detection of Fe(III). J Mater Sci 50:2571–2576. doi:10.1007/s10853-015-8822-6
12. Xu X, Ray R, Gu Y, Ploehn HJ, Gearheart L, Raker K et al (2004) Electrophoretic analysis and purification of fluorescent single-walled carbon nanotube fragments. J Am Chem Soc 126:12736–12737
13. Xu MH, He GL, Li ZH, He FJ, Gao F, Su YJ, Zhang LY, Yang Z, Zhang YF (2014) A green heterogeneous synthesis of N-doped carbon dots and their photoluminescence applications in solid and aqueous states. Nanoscale 6:10307–10315
14. Sun D, Ban R, Zhang PH, Wu GH, Zhang JR, Zhu JJ (2013) Hair fiber as a precursor for synthesizing of sulfur- and nitrogen-co-doped carbon dots with tunable luminescence properties. Carbon 64:424–434
15. Wang XH, Qu KG, Xu BL, Ren JS, Qu XG (2011) Microwave assisted one-step green synthesis of cell-permeable multicolor photoluminescent carbon dots without surface passivation reagents. J Mater Chem 21:2445–2450
16. Zhuo S, Shao M, Lee S-T (2012) Upconversion and downconversion fluorescent graphene quantum dots: ultrasonic preparation and photocatalysis. ACS Nano 6:1059–1064
17. Li XY, Wang HQ, Shimizu Y, Pyatenko A, Kawaguchi K, Koshizaki N (2011) Preparation of carbon quantum dots with tunable photoluminescence by rapid laser passivation in ordinary organic solvents. Chem Commun 47:932–934
18. Deng JH, Lu QJ, Mi NX, Li HT, Liu ML, Xu MC, Tan L, Xie QJ, Zhang YY, Yao SZ (2014) Electrochemical synthesis of carbon nanodots directly from alcohols. Chem Eur J 20:4993–4999
19. Antonietti M, Kuang DB, Smarsly B, Zhou Y (2004) Ionic liquids for the convenient synthesis of functional nanoparticles and other inorganic nanostructures. Angew Chem Int Ed 43:4988–4992
20. Chen YM, Chen MM, Shi JC, Yang J, Zhang DF (2014) Fabrication of "clean" nano-structured metal materials on ionic liquid/water interface. Mater Lett 132:153–156
21. Smiglak M, Pringle JM, Lu X, Han L, Zhang S, Gao H, MacFarlane DR, Rogers RD (2014) Ionic liquids for energy, materials, and medicine. Chem Commun 50:9228–9250
22. Lu J, Yang JX, Wang JZ, Lim AL, Wang S, Loh KP (2009) One–pot synthesis of fluorescent carbon nanoribbons, nanoparticles, and graphene by the exfoliation of graphite in ionic liquids. ACS Nano 3:2367–2375
23. Li XH, Zhao ZW (2014) Facile ionic-liquid-assisted electrochemical synthesis of size-controlled carbon quantum dots by tuning applied voltages. RSC Adv 4:57615–57619
24. Zhao AD, Zhao CQ, Li M, Ren JS, Qu XG (2014) Ionic liquids as precursors for highly luminescent, surface-different nitrogen-doped carbon dots used for label-free detection of Cu^{2+}/Fe^{3+} and cell imaging. Anal Chim Acta 809:128–133
25. Wang BG, Tang WW, Lu HS, Huang ZY (2015) Hydrothermal synthesis of ionic liquid-capped carbon quantum dots with high thermal stability and anion responsiveness. J Mater Sci 50:5411–5418. doi:10.1007/s10853-015-9085-y
26. Hajipour AR, Rafiee F (2010) Acidic Bronsted Ionic Liquids. Org Prep Proced Int 42:285–362
27. Liu YY, Xiao WW, Xia SQ, Ma PS (2013) SO_3H-functionalized acidic ionic liquids as catalysts for the hydrolysis of cellulose. Carbohydr Polym 92:218–222
28. Ohno H, Fukaya Y (2009) Task specific ionic liquids for cellulose technology. Chem Lett 38:2–7
29. Wang H, Gurau G, Rogers RD (2012) Ionic liquid processing of cellulose. Chem Soc Rev 4:1519–1537
30. Chheda JN, Huber GW, Dumesic JA (2007) Liquid-phase catalytic processing of biomass-derived oxygenated hydrocarbons to fuels and chemicals. Angew Chem Int Ed 46:7164–7183
31. Tao FR, Song HL, Chou LJ (2011) Hydrolysis of cellulose in SO_3H-functionalized ionic liquids. Bioresour Technol 102:9000–9006
32. Hu YP, Yang J, Jia L, Yu JS (2015) Ethanol in aqueous hydrogen peroxide solution: hydrothermal synthesis of highly photoluminescent carbon dots as multifunctional nanosensors. Carbon 93:999–1007
33. Yan HP, Tan MQ, Zhang DM, Cheng FS, Wu H, MK Fan, Ma XJ, Wang JH (2013) Development of multicolor carbon nanoparticles for cell imaging. Talanta 108:59–65
34. Liu NY, Liu J, Kong WQ, Li H, Huang H, Liu Y, Kang ZH (2014) One-step catalase controllable degradation of C_3N_4 for N-doped carbon dot green fabrication and their bioimaging applications. J Mater Chem B 2:5768–5774
35. Yang XM, Zhuo Y, Zhu SS, Luo YW, Feng YJ, Dou Y (2014) Novel and green synthesis of high-fluorescent carbon dots originated from honey for sensing and imaging. Biosens Bioelectron 60:292–298
36. Liu YS, Zhao YA, Zhang YY (2014) One-step green synthesized fluorescent carbon nanodots from bamboo leaves for copper(II) ion detection. Sens Actuators, B 196:647–652
37. Zhu SJ, Song YB, Zhao XH, Shao JR, Zhang JH, Yang B (2015) The photoluminescence mechanism in carbon dots (graphene quantum dots, carbon nanodots, and polymer dots): current state and future perspective. Nano Res 8:355–381
38. Yang Z, Xu MH, Liu Y, He FJ, Gao F, Su YJ, Wei H, Zhang YF (2014) Nitrogen-doped, carbon-rich, highly photoluminescent carbon dots from ammonium citrate. Nanoscale 6:1890–1895
39. Xia YS, Zhu CQ (2008) Use of surface-modified CdTe quantum dots as fluorescent probes in sensing mercury (II). Talanta 75:215–221
40. Hatai J, Pal S, Jose GP, Bandyopadhyay S (2012) Histidine based fluorescence sensor detects Hg^{2+} in solution, paper strips, and in cells. Inorg Chem 51:10129–10135